

Coulomb drag between two strange metals

E. Mauri* and H.T.C. Stoof†

*Institute for Theoretical Physics and Center for Extreme Matter and Emergent Phenomena,
Utrecht University, Princetonplein 5, 3584 CC Utrecht, The Netherlands*

We study the Coulomb drag between two strange-metal layers using the Einstein-Maxwell-Dilaton model from holography. We show that the low-temperature dependence of the drag resistivity is $\rho_D \propto T^4$, which strongly deviates from the quadratic dependence of Fermi liquids. We also present numerical results at room temperature, using typical parameters of the cuprates, to provide an estimate of the magnitude of this effect for future experiments. We find that the drag resistivity is enhanced by the plasmons characteristic of the two-layer system.

Introduction. — The cuprates have been of interest to both the experimental and theoretical physics community for the past three decades due to their peculiar metallic properties that cannot be explained within the standard Fermi-liquid framework [1, 2]. In this class of materials, that have in common a layered structure of CuO_2 planes, strong Coulomb interactions between the electrons give rise to unusual and still unclear quantum behavior, of which the high-temperature superconducting phase is of most technological importance. Above the maximum critical temperature of the superconducting phase, we find the so-called strange metal, whose anomalous linear-in- T resistivity [3–8] characterizes its non-Fermi liquid behavior, even if the superconductivity is suppressed by a magnetic field [9]. Given the importance of understanding the physics at play in the strange-metal phase in order to also get a better grasp on the instability towards high-temperature superconductivity, there have been a variety of attempts to model the strongly interacting cuprates [10–19]. One technique in particular is the application of the AdS/CFT correspondence, or holographic duality [20], conjectured and first developed by the string-theory community, but that has proven to be a powerful tool to qualitatively study low-energy properties of strongly interacting quantum matter as well [21–23].

In this Letter we use a holographic Einstein-Maxwell-Dilaton model of the strange metal [24] to study a two-layer system where the interaction among the different layers is only mediated by the long-range Coulomb force. The importance of such a setting is motivated by the experimental relevance of multi-layered systems. For simplicity most of the holographic studies of the cuprates focus on describing the behavior of a single-layer, however, there has been recent experimental interests in probing also the bulk response of the cuprates [25, 26]. Experimental results in both hole- and electron-doped cuprates show that the density response is governed by the inter-layer Coulomb interaction, giving rise to low-energy acoustic plasmon modes. Plasmons are ubiquitous in condensed-matter materials due to the electric charge of the electron, but only recently a way to capture the charged nature of the system has been proposed in holography [27–31], opening the door to the possibility

of studying ‘holographic’ plasmons and providing a simplified framework to test experimental results on acoustic plasmons in multi-layered cuprates [30].

In view of these developments, our main aim is here to present a link between holographic predictions and experimental results by studying the density response of two holographic strange-metal layers. In particular, by considering the Coulomb drag resistivity, we are able to obtain also quantitative estimates of the drag effect in the hope to provide a verifiable prediction to either validate the holographic model or to show its shortcomings. Here Coulomb drag refers to a transport phenomenon of a system of closely spaced but electrically isolated layers, where a current driven through the ‘active’ layer gives rise to a current in the nearby ‘passive’ layer due to inter-layer scattering of the charge carriers mediated by the long-range Coulomb interaction that couples density fluctuations among the different layers [32]. A typical experimental set-up is shown in Fig. 1, where a known current is driven through one layer and the drag effect, parametrized by the drag resistivity ρ_D , is studied by

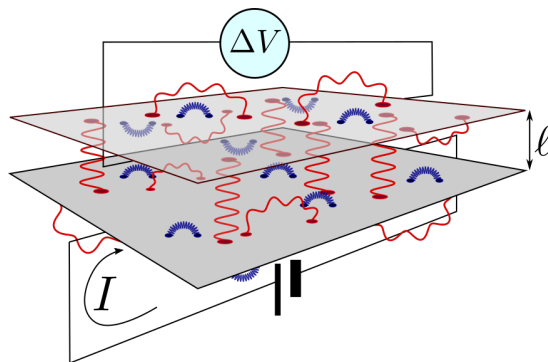


FIG. 1: Experimental set-up for a Coulomb drag measurement. A current I flows through the active layer and the voltage drop $\Delta V = -R_D I$ induced in the passive layer is observed to measure the drag resistance. In the holographic description under study we have two types of interactions, i.e., strong in-plane interactions leading to strange-metal behavior (blue) and the long-range Coulomb interactions (red).

measuring the voltage drop in the passive layer.

In the holographic description we are using, the system is characterized by two kinds of interactions, a strong one that is of short range and therefore does not contribute to the inter-layer scattering, and the long-range Coulomb interaction that instead also gives rise to the coupling between the separate layers. The success of the holographic duality relies on the fact that it naturally describes a strongly interacting system, such as a strange metal [33], and we thus can take two copies of such a model to describe the two layers. On the other hand, it is important to realize that holographic models present always a ‘neu-

tral’ response, where there are no photons in the system. However, by performing a so-called double-trace deformation [34], we have recently shown how to add within holography also the long-range Coulomb screening effects to multi-layered models on top of the strong neutral interactions [30]. We use this procedure here to couple the holographic strange-metal layers in order to study the Coulomb drag resistivity, as we explain in detail in the following.

Coulomb drag resistivity. — Our starting point is the drag resistivity within the random-phase approximation that is given by the expression [35–38]

$$\rho_D = \frac{\hbar^2}{16\pi^3 e^2 n_1 n_2 k_B T} \int_{-\infty}^{+\infty} \frac{d\omega}{\sinh^2(\hbar\omega/2k_B T)} \int d\mathbf{q} \mathbf{q}^2 \frac{\text{Im}[\Pi_1(\omega, \mathbf{q})]}{|\Pi_1(\omega, \mathbf{q})|^2} |\chi_{12}(\omega, \mathbf{q})|^2 \frac{\text{Im}[\Pi_2(\omega, \mathbf{q})]}{|\Pi_2(\omega, \mathbf{q})|^2}, \quad (1)$$

where n_1 and n_2 are the densities of the active and passive layers, respectively, $\Pi_i(\omega, \mathbf{q})$ are the corresponding intra-layer density-density response functions, and the dynamically screened inter-layer density response is given by

$$\chi_{12} = -\frac{\Pi_1 \Pi_2^*}{\Pi_1 \Pi_2 \frac{e^2}{\epsilon q} \sinh(q\ell) + \left[\frac{2q\epsilon}{e^2} - \Pi_1 - \Pi_2\right] e^{q\ell}}, \quad (2)$$

with $q = |\mathbf{q}|$, ℓ the separation between the two layers, and ϵ the dielectric constant of the insulating material surrounding the layers. This approximation ignores the effect of vertex corrections. However, it has been observed experimentally that the electron self-energy in the cuprates depends mostly on frequency. This feature is also captured in our holographic model where the low-energy theory is described by a ‘semi-local’ quantum critical phase, where the electron self-energy $\hbar\Sigma(\omega, \mathbf{k})$ scales like $\omega^{2\nu_k}$, with the momentum dependence only entering in the power ν_k [24, 39]. We therefore expect Eq. (1) to be a valid approximation for the Coulomb drag resistivity for a cuprate two-layer system in the strange-metal regime.

From Eqs. (1) and (2) we see that the only input we need to compute the drag resistivity are the single-layer response functions $\Pi_i(\omega, \mathbf{q})$. The power of our holographic approach now lies in the fact that it allows us to compute this response in a strongly interacting system. Since the behavior of the drag resistivity depends solely on the nature of the inter-layer interactions, and not on disorder, it may reveal interesting features of the cuprates, and possibly verify if the proposed holographic model of the strange metal correctly describes this phenomenon.

Einstein-Maxwell-Dilaton theory. — Let us briefly review how we obtain the strange-metal response func-

tion from holography. The holographic duality states the equivalence between a strongly interacting quantum theory and a classical gravitational theory with one additional spatial dimension, where the coordinate r of this additional dimension parametrizes the energy scale of the quantum field theory. In particular low-energy physics is described by the geometry in the deep interior ($r \rightarrow 0$) of the spacetime, while the near-boundary geometry ($r \rightarrow \infty$) characterize the ultra-violet details of the dual field theory. The thermodynamics of the holographic strange-metal model proposed by Gubser *et al.* [24], is described by a solution to the coupled set of Einstein equations for the metric $g_{\mu\nu}$, Maxwell equations for the $U(1)$ gauge field A_μ , and the Klein-Gordon equation for the real scalar field ϕ , known as the dilaton [40, 41]:

$$\begin{aligned} R_{\mu\nu} - \frac{1}{2} R g_{\mu\nu} &= T_{\mu\nu}, \quad \nabla_\mu (e^{\phi/\sqrt{3}} F^{\mu\nu}) = 0, \\ \nabla_\mu \nabla^\mu \phi &= \frac{e^{\phi/\sqrt{3}}}{4\sqrt{3}} F^2 - \frac{2\sqrt{3}}{L^2} \sinh(\phi/\sqrt{3}), \end{aligned} \quad (3)$$

where $R_{\mu\nu}$ and R are the Ricci tensor and scalar, respectively, and the energy-momentum tensor equals

$$\begin{aligned} T_{\mu\nu} &= \frac{1}{2} \partial_\mu \phi \partial_\nu \phi + \frac{e^{\phi/\sqrt{3}}}{2} F_\mu^\sigma F_{\nu\sigma} \\ &- g_{\mu\nu} \left(\frac{e^{\phi/\sqrt{3}}}{8} F^2 + \frac{(\partial_\sigma \phi)^2}{4} + \frac{3}{L^2} \cosh(\phi/\sqrt{3}) \right). \end{aligned} \quad (4)$$

Finally, $F_{\mu\nu} = \partial_\mu A_\nu - \partial_\nu A_\mu$ is the field strength and L is the AdS radius. In particular, as we are interested in a regime where the underlying lattice structure of the cuprates does not play a role in the drag resistivity, the fields in Eq. (3) are a function of the radial coordinate r only. This set of equations for ($g_{tt} = -1/g_{rr}, g_{xx} = g_{yy}, A_t, \phi$) then support a fully analytical black-hole so-

lution [24], with a non-zero temperature and entropy, and with $A_t(r)$ setting a non-zero density in the dual boundary theory through the radially conserved quantity $n \equiv \sqrt{-g(r)} e^{\phi(r)/\sqrt{3}} F^{rt}(r)$, $g(r)$ being the determinant of the metric.

The dilaton field is such that the emergent low-energy theory is described by a semi-local quantum critical phase with both the dynamical critical exponent $z = \infty$ and the hyperscaling violation exponent $\theta = -\infty$ divergent but with a fixed ratio equal to -1 . The dynamical exponent $z = \infty$ implies that at energies well below the Fermi energy, quantum critical correlations can only depend on momentum through the power of the frequency dependence, while $\theta/z = -1$ ensures that the entropy goes linearly to zero at zero temperature [21]. Ultimately, this scaling allows for the description of a quantum critical phase with a linear-in- T resistivity [39] and an electron self-energy that is dominated by its frequency dependence as desired for a strange metal [42].

In order to also compute the response of the holographic strange metal to small external perturbations, we have to linearize the gravitational equations in Eq. (3) around the black-hole solution. We obtain in this way a set of coupled equations for the fluctuations $(\delta g_{tt}, \delta g_{tx}, \delta g_{xx}, \delta g_{yy}, \delta A_t, \delta A_x, \delta \phi)$ that can only be solved numerically. According to the holographic dictionary [21–23, 33], finding such a solution with infalling-wave boundary conditions at the black-hole horizon, allows us to extract all the retarded Green's function of the system, and hence the density-density response function $\Pi(\omega, \mathbf{q})$, by studying the near-boundary behavior of the field fluctuations.

Results. — We work in each layer with electrons at the same fixed equilibrium density n , and we study the holographic density response function, that is anticipated to describe the physics of the strange metal near the Fermi momentum in the regime where the dispersion of the electrons can be linearized. Therefore we replace from now on the speed of light in the gravitational theory with the Fermi velocity, i.e., $c \rightarrow v_F$. In the low-temperature regime and at energies and momenta much smaller than the Fermi energy and Fermi momentum, respectively, we find that the response function is well approximated by a hydrodynamic model of the form [43]

$$\Pi(\omega, q) = \frac{q^2 (\omega \mathcal{D} + i v_s^2 D_d \chi q^2)}{\omega^3 + i \omega^2 q^2 (2D_s + D_d) - \omega q^2 v_s^2 - i v_s^2 D_d q^4} \quad (5)$$

that contains a linear sound mode at $\omega = \pm v_s q - i D_s q^2 + \mathcal{O}(q^4)$, and a diffusive mode at $\omega = -i D_d q^2 + \mathcal{O}(q^4)$, with \mathcal{D} the Drude weight, and $\chi = -\lim_{q \rightarrow 0, \omega \rightarrow 0} \Pi(\omega, \mathbf{q})$ the (hydrodynamic) compressibility. This form of Π implies that the integrand in Eq. (1) contains, for our symmet-

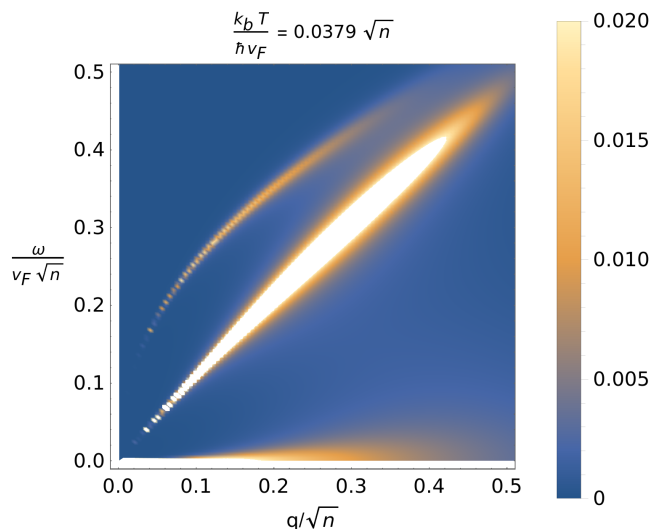


FIG. 2: Typical integrand in Eq. (1), normalized to peak height, showing the in-phase and out-of phase plasmon modes, and the low-energy diffusive mode.

ric case $\Pi_i \equiv \Pi$ (it is straightforward to generalize the results to layers with different densities and three different surrounding dielectric constants [44]), in addition to a diffusive mode $\omega = -i D_d q^2$, the out-of-phase acoustic plasmon mode and the in-phase optical plasmon characteristic of a two-layer system [44–48]. The latter frequencies are

$$\omega = \pm \sqrt{v_s^2 + \frac{e^2 \mathcal{D} \ell}{2\epsilon}} q + \mathcal{O}(q^2) \quad (6)$$

$$\omega = \pm \sqrt{\frac{e^2 \mathcal{D} q}{\epsilon}} \left(1 + \frac{v_s^2 - e^2 \mathcal{D} \ell / 2\epsilon}{2e^2 \mathcal{D} / \epsilon} q \right) + \mathcal{O}(q^2) . \quad (7)$$

All three modes are clearly visible in the numerical result for the integrand in Fig. 2. These modes thus determine the low-temperature behavior of the drag resistivity. We emphasize here that compared to a purely hydrodynamic approach as in Refs. [49, 50], the holographic model gives also a prediction for the coefficients in Eq. (5) and for their temperature dependence, allowing us to fully determine the dominant low-temperature behavior of ρ_D . In particular, we numerically explored the pole structure of the retarded density correlators in the limit of $T \rightarrow 0$ to find that in this low-temperature hydrodynamics [51–53], the sound diffusion coefficient equals $D_s = (1/6\sqrt{3}) k_B T / \hbar n$, whereas the other diffusion constant obeys [21] $D_d = (4\pi/\sqrt{3}) k_B T / \hbar n$. Both are fully determined by background (thermodynamic) quantities, as is the zero-temperature Drude weight $\mathcal{D} = (1/3^{1/4}) v_F \sqrt{n} / \hbar$. We further find a speed of sound, that differs from the $v_F / \sqrt{2}$ of a conformal field theory as conformal invariance is broken in the low-energy limit by the dilaton field. We obtain $v_s \approx 0.76 v_F$, that is

slightly higher than expected from the thermodynamic potential Ω via $v_s = (-\partial\Omega/\partial\epsilon)^{1/2} = \sqrt{17/31}v_F$. Accordingly, $\chi = \mathcal{D}/v_s^2 \approx 1.32\sqrt{n}/\hbar v_F$ so that the height of the diffusive peak is determined by the subleading behavior $(\mathcal{D}/v_s^2 - \chi)/2 \approx 2.56T^2/\sqrt{n}(\hbar v_F)^3$, with the proportionality constant obtained numerically.

The hydrodynamic model in Eq. (5), together with the above results, can be integrated to compute the drag resistivity according to Eq. (1). Doing so shows that in the low-temperature limit and $e^2\chi\ell/\epsilon \gg 1$ the behavior is dominated by the diffusive mode, that implies $\rho_D(T) \propto T^4$, strikingly different from the Fermi liquid result $\rho_D(T) \propto T^2$ due to thermal broadening of the Fermi surface [35, 36, 54]. By considering the diffusive mode alone in Eq. (5), using that in the limits of interest $\Pi \approx \chi$, the drag resistivity can be determined analytically to yield

$$\rho_D = \frac{3\zeta(3)}{32\pi^2} \frac{\hbar}{e^2} \frac{(\mathcal{D}/v_s^2 - \chi)^2}{\chi^2 n \ell^2 (e^2 \chi \ell / \epsilon)^2} \propto \frac{T^4}{\ell^4}. \quad (8)$$

For the cuprates ($e^2\chi\ell/\epsilon \approx 2.6$) the full hydrodynamic result is considerable larger than expected from diffusion alone but has the same temperature dependence as shown in the inset of Fig. 3. It is important to notice that the temperature dependence of the dissipative coefficients D_d and D_s is characteristic of the particular holographic model used. However, the linear dependence on T of these coefficients comes from the linear-in- T resistivity, that is a fundamental requirement of any strange-metal model. We would also like to highlight that, due to the introduction of the Coulomb interactions into the holographic model, we are able to obtain also the magnitude of the drag effect. In a bottom-up approach to holography we are only able to compute response func-

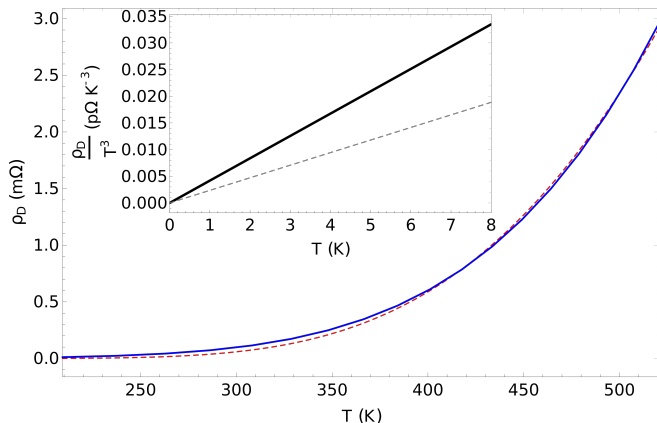


FIG. 3: Coulomb drag at high temperature (blue), where it is determined by the plasmons, together with the fit $\rho_D \propto e^{-\Delta/T}$ and $\Delta \approx 2760$ K (dashed red). In the inset the low-temperature results obtained from hydrodynamics (black) and diffusion only (dashed grey).

tions up to an unknown factor related to (dimensionless) Newton's constant $16\pi G\hbar/c^3 L^2$. The introduction of the Coulomb interaction, and hence the plasma frequency, allows us to match this unknown constant with the experimentally observed plasma frequency and uniquely fix the magnitude of the density response.

For the curves given in Fig. 3, we use the density $n = 7.1 \times 10^{14} \text{ cm}^{-2}$, the Fermi velocity obeying $\hbar v_F = 3 \text{ eV\AA}$ as typical in the cuprates, and the inter-layer spacing $\ell = 7.5 \text{ \AA}$ that is of the order of the effective inter-layer distance of LCCO planes used in the experiment on plasmons by Hepting *et al.* [25]. In addition, a value of the above-mentioned overall constant equal to one and also $e^2/\epsilon\hbar v_F = 1$ turns out to give a plasmon dispersion of the same magnitude as observed in this experiment. For this choice of parameters, the low-temperature hydrodynamic behavior gives a very small resistivity. However, we numerically considered also temperatures at and above room temperature. Here we are in a regime that lies outside the region of validity of the hydrodynamic model in Eq. (5), and the dominant contribution to the drag resistivity comes from higher energies where the acoustic plasmon, and to a lesser extent the optical plasmon, play a major role in the magnitude of the effect. In this regime the temperature behavior is mostly due to the thermal factor $1/\sinh^2(\hbar\omega/2k_B T)$ in Eq. (1) and hence it gives an exponential growth, leading to a resistivity of similar magnitude as in drag experiments with two-dimensional electron gases.

Conclusion and outlook. — We have here studied by holography the Coulomb drag between two strange metals and have shown how to determine the drag resistivity in such a strongly interacting system. We performed the computation within a particular model for which an analytical background solution exists and showed the important role of the linear acoustic plasmon mode in the drag resistivity at easily accessible temperatures.

The holographic model used captures various qualitative features of the low-energy properties of the strange metal. However, we also have to keep in mind that it describes a system with a very different ultra-violet behavior compared to a laboratory cuprate material as the electronic dispersion is implicitly linearized and no lattice band-structure is involved in the calculation. This may affect the quantitative estimate of the drag resistivity somewhat. A important matter of future studies is the thermodynamics of the strange metal, as an analytical understanding of the observed values for the speed of sound and susceptibility is still lacking. We, nevertheless, hope that the theory presented here may stimulate further experiments on drag transport to test holographic quantum matter in general and strange metals in particular.

Acknowledgments. — We are grateful to Alberto Cortijo for helpful suggestions and discussions. This work

is supported by the Stichting voor Fundamenteel Onderzoek der Materie (FOM) and is part of the D-ITP consortium, a program of the Netherlands Organization for Scientific Research (NWO) that is funded by the Dutch Ministry of Education, Culture and Science (OCW).

* E.Mauri@uu.nl

† H.T.C.Stoof@uu.nl

- [1] C. Proust and L. Taillefer, The remarkable underlying ground states of cuprate superconductors, *Annual Review of Condensed Matter Physics* **10**, 409 (2019).
- [2] B. Keimer, S. A. Kivelson, M. R. Norman, S. Uchida, and J. Zaanen, From quantum matter to high-temperature superconductivity in copper oxides, *Nature* **518**, 179 (2015).
- [3] J. Custers, P. Gegenwart, H. Wilhelm, K. Neumaier, Y. Tokiwa, O. Trovarelli, C. Geibel, F. Steglich, C. Pépin, and P. Coleman, The break-up of heavy electrons at a quantum critical point, *Nature* **424**, 524 (2003).
- [4] R. A. Cooper, Y. Wang, B. Vignolle, O. J. Lipscombe, S. M. Hayden, Y. Tanabe, T. Adachi, Y. Koike, M. Nohara, H. Takagi, C. Proust, and N. E. Hussey, Anomalous criticality in the electrical resistivity of $\text{La}_{2-x}\text{Sr}_x\text{CuO}_4$, *Science* **323**, 603 (2009).
- [5] J. A. N. Bruin, H. Sakai, R. S. Perry, and A. P. Mackenzie, Similarity of Scattering Rates in Metals Showing T-Linear Resistivity, *Science* **339**, 804 (2013).
- [6] J. G. Analytis, H.-H. Kuo, R. D. McDonald, M. Wartenbe, P. M. C. Rourke, N. E. Hussey, and I. R. Fisher, Transport near a quantum critical point in $\text{BaFe}_2(\text{As}_{1-x}\text{Px})_2$, *Nature Physics* **10**, 194 (2014).
- [7] A. Legros, S. Benhabib, W. Tabis, F. Laliberté, M. Dion, M. Lizaire, B. Vignolle, D. Vignolles, H. Raffy, Z. Z. Li, P. Auban-Senzier, N. Doiron-Leyraud, P. Fournier, D. Colson, L. Taillefer, and C. Proust, Universal t-linear resistivity and planckian dissipation in overdoped cuprates, *Nature Physics* **15**, 142 (2018).
- [8] S. Licciardello, J. Buhot, J. Lu, J. Ayres, S. Kasahara, Y. Matsuda, T. Shibauchi, and N. E. Hussey, Electrical resistivity across a nematic quantum critical point, *Nature* **567**, 213 (2019).
- [9] N. E. Hussey, J. Buhot, and S. Licciardello, A tale of two metals: contrasting criticalities in the pnictides and hole-doped cuprates, *Reports on Progress in Physics* **81**, 052501 (2018).
- [10] P. A. Lee, N. Nagaosa, and X.-G. Wen, Doping a mott insulator: Physics of high-temperature superconductivity, *Rev. Mod. Phys.* **78**, 17 (2006).
- [11] M. Ogata and H. Fukuyama, The t-j model for the oxide high- T_c superconductors, *Reports on Progress in Physics* **71**, 036501 (2008).
- [12] H. Mukuda, S. Shimizu, A. Iyo, and Y. Kitaoka, High- T_c superconductivity and antiferromagnetism in multilayered copper oxides – a new paradigm of superconducting mechanism –, *Journal of the Physical Society of Japan* **81**, 011008 (2012).
- [13] Y. Kakehashi and P. Fulde, Marginal fermi liquid theory in the hubbard model, *Phys. Rev. Lett.* **94**, 156401 (2005).
- [14] J. Kokalj, N. E. Hussey, and R. H. McKenzie, Transport properties of the metallic state of overdoped cuprate superconductors from an anisotropic marginal fermi liquid model, *Phys. Rev. B* **86**, 045132 (2012).
- [15] J. Zaanen, O. Y. Osman, H. Eskes, and W. van Saarloos, Dynamical stripe correlations in cuprate superconductors, *Journal of Low Temperature Physics* **105**, 569 (1996).
- [16] V. J. Emery, S. A. Kivelson, and J. M. Tranquada, Stripe phases in high-temperature superconductors, *Proceedings of the National Academy of Sciences* **96**, 8814 (1999).
- [17] E. Berg, E. Fradkin, S. A. Kivelson, and J. M. Tranquada, Striped superconductors: how spin, charge and superconducting orders intertwine in the cuprates, *New Journal of Physics* **11**, 115004 (2009).
- [18] M. Vojta, Lattice symmetry breaking in cuprate superconductors: stripes, nematics, and superconductivity, *Advances in Physics* **58**, 699 (2009).
- [19] Y. Zhang, C. Lane, J. W. Furness, B. Barbiellini, J. P. Perdew, R. S. Markiewicz, A. Bansil, and J. Sun, Competing stripe and magnetic phases in the cuprates from first principles, *Proceedings of the National Academy of Sciences* **117**, 68 (2020).
- [20] J. Maldacena, The large- n limit of superconformal field theories and supergravity, *International Journal of Theoretical Physics* **38**, 1113 (1999).
- [21] S. A. Hartnoll, A. Lucas, and S. Sachdev, *Holographic quantum matter* (2016).
- [22] J. Zaanen, Y. Liu, Y.-W. Sun, and K. Schalm, *Holographic Duality in Condensed Matter Physics* (Cambridge University Press, 2015).
- [23] M. Ammon and J. Erdmenger, *Gauge/Gravity Duality: Foundations and Applications* (Cambridge University Press, 2015).
- [24] S. S. Gubser and F. D. Rocha, Peculiar properties of a charged dilatonic black hole in ads_5 , *Phys. Rev. D* **81**, 046001 (2010).
- [25] M. Hepting, L. Chaix, E. W. Huang, R. Fumagalli, Y. Y. Peng, B. Moritz, K. Kummer, N. B. Brookes, W. C. Lee, M. Hashimoto, T. Sarkar, J.-F. He, C. R. Rotundu, Y. S. Lee, R. L. Greene, L. Braicovich, G. Ghiringhelli, Z. X. Shen, T. P. Devereaux, and W. S. Lee, Three-dimensional collective charge excitations in electron-doped copper oxide superconductors, *Nature* **563**, 374 (2018).
- [26] A. Nag, M. Zhu, M. Bejas, J. Li, H. C. Robarts, H. Yamase, A. N. Petsch, D. Song, H. Eisaki, A. C. Walters, M. García-Fernández, A. Greco, S. M. Hayden, and K.-J. Zhou, Detection of acoustic plasmons in hole-doped lanthanum and bismuth cuprate superconductors using resonant inelastic x-ray scattering, *Phys. Rev. Lett.* **125**, 257002 (2020).
- [27] U. Gran, M. Tornsö, and T. Zingg, Holographic plasmons, *Journal of High Energy Physics* **2018**, 176 (2018).
- [28] U. Gran, M. Tornsö, and T. Zingg, Plasmons in Holographic Graphene, *SciPost Phys.* **8**, 93 (2020).
- [29] U. Gran, M. Tornsö, and T. Zingg, Exotic holographic dispersion, *Journal of High Energy Physics* **2019**, 32 (2019).
- [30] E. Mauri and H. T. C. Stoof, Screening of coulomb interactions in holography, *Journal of High Energy Physics* **2019**, 35 (2019).
- [31] A. Romero-Bermúdez, A. Krikun, K. Schalm, and J. Zaanen, Anomalous attenuation of plasmons in strange metals and holography, *Phys. Rev. B* **99**, 235149 (2019).
- [32] B. N. Narozhny and A. Levchenko, Coulomb drag, *Rev.*

- Mod. Phys. **88**, 025003 (2016).
- [33] S. A. Hartnoll, Lectures on holographic methods for condensed matter physics, *Classical and Quantum Gravity* **26**, 224002 (2009).
- [34] E. Witten, Multi-trace operators, boundary conditions, and ads/cft correspondence, arXiv (2002).
- [35] A.-P. Jauho and H. Smith, Coulomb drag between parallel two-dimensional electron systems, *Phys. Rev. B* **47**, 4420 (1993).
- [36] L. Zheng and A. H. MacDonald, Coulomb drag between disordered two-dimensional electron-gas layers, *Phys. Rev. B* **48**, 8203 (1993).
- [37] K. Flensberg, B. Y.-K. Hu, A.-P. Jauho, and J. M. Kinaret, Linear-response theory of coulomb drag in coupled electron systems, *Phys. Rev. B* **52**, 14761 (1995).
- [38] A. Kamenev and Y. Oreg, Coulomb drag in normal metals and superconductors: Diagrammatic approach, *Physical Review B* **52**, 7516 (1995).
- [39] R. J. Anantua, S. A. Hartnoll, V. L. Martin, and D. M. Ramirez, The pauli exclusion principle at strong coupling: holographic matter and momentum space, *Journal of High Energy Physics* **2013**, 104 (2013).
- [40] C. Charmousis, B. Goutéraux, B. Soo Kim, E. Kiritsis, and R. Meyer, Effective holographic theories for low-temperature condensed matter systems, *Journal of High Energy Physics* **2010**, 151 (2010).
- [41] B. Goutéraux and E. Kiritsis, Generalized holographic quantum criticality at finite density, *Journal of High Energy Physics* **2011**, 36 (2011).
- [42] S. S. Gubser and J. Ren, Analytic fermionic green's functions from holography, *Phys. Rev. D* **86**, 046004 (2012).
- [43] P. Kovtun, Lectures on hydrodynamic fluctuations in relativistic theories, *Journal of Physics A: Mathematical and Theoretical* **45**, 473001 (2012).
- [44] S. M. Badalyan and F. M. Peeters, Enhancement of coulomb drag in double-layer graphene structures by plasmons and dielectric background inhomogeneity, *Phys. Rev. B* **86**, 121405 (2012).
- [45] E. H. Hwang and S. Das Sarma, Plasmon modes of spatially separated double-layer graphene, *Phys. Rev. B* **80**, 205405 (2009).
- [46] T. Vazifeshenas, T. Amlaki, M. Farmanbar, and F. Parhizgar, Temperature effect on plasmon dispersions in double-layer graphene systems, *Physics Letters A* **374**, 4899 (2010).
- [47] R. E. V. Profumo, R. Asgari, M. Polini, and A. H. MacDonald, Double-layer graphene and topological insulator thin-film plasmons, *Phys. Rev. B* **85**, 085443 (2012).
- [48] T. Stauber and G. Gómez-Santos, Plasmons and near-field amplification in double-layer graphene, *Phys. Rev. B* **85**, 075410 (2012).
- [49] S. S. Apostolov, A. Levchenko, and A. V. Andreev, Hydrodynamic coulomb drag of strongly correlated electron liquids, *Phys. Rev. B* **89**, 121104 (2014).
- [50] T. Holder, Hydrodynamic coulomb drag and bounds on diffusion, *Phys. Rev. B* **100**, 235121 (2019).
- [51] M. Edalati, J. I. Jottar, and R. G. Leigh, Holography and the sound of criticality, *Journal of High Energy Physics* **2010**, 58 (2010).
- [52] A. Karch, D. T. Son, and A. O. Starinets, Holographic quantum liquid, *Phys. Rev. Lett.* **102**, 051602 (2009).
- [53] R. A. Davison and N. K. Kaplis, Bosonic excitations of the ads4 reissner-nordstrom black hole, *Journal of High Energy Physics* **2011**, 37 (2011).
- [54] T. J. Gramila, J. P. Eisenstein, A. H. MacDonald, L. N. Pfeiffer, and K. W. West, Mutual friction between parallel two-dimensional electron systems, *Phys. Rev. Lett.* **66**, 1216 (1991).